Spectroscopic and Thermodynamic Studies of DNA Duplexes Containing α-Anomeric C, A, and G Nucleotides and Polarity Reversals: Coexistence of Localized Parallel and Antiparallel DNA†

James M. Aramini,‡ Johan H. van de Sande,§ and Markus W. Germann*,‡

Department of Microbiology and Immunology, Kimmel Cancer Institute, Thomas Jefferson University, Philadelphia, Pennsylvania 19107, and Department of Medical Biochemistry, University of Calgary, Calgary, Alberta, Canada T2N 4N1

Received March 17, 1997; Revised Manuscript Received May 29, 1997⊗

ABSTRACT: We present a thermodynamic, enzymatic, and spectroscopic study of three self-complementary DNA decamer duplexes, d[GCGAATT-3′−3′-(αC)-5′−5′-GC]$_2$ (alphaC), d[GCG-3′−3′-(αA)-5′−5′-ATTCGC]$_2$ (alphaA), and d[GC-3′−3′-(αG)-5′−5′-AATTCGC]$_2$ (alphaG), which are identical in sequence but contain one α-anomeric nucleotide per strand in a parallel orientation via 3′−3′ and 5′−5′ phosphodiester bonds; the results are placed in the context of our recent studies on the other members of this series, namely alphaT, d[GCGAAT-3′−3′-(αT)-5′−5′-CGC]$_2$, and the unmodified control [Aramini, J. M., et al. (1996) *Biochemistry 35*, 9355−9365]. On the basis of UV hyperchromicity and melting profiles as well as ^{1}H and ^{31}P nuclear magnetic resonance (NMR) spectroscopic data, we conclude that all five constructs form stable duplexes, with very comparable structural features that are consistent with an overall right-handed, antiparallel B-DNA motif and Watson−Crick base pairing throughout. However, each of the α-containing sequences exhibits unique thermodynamic and structural differences ascribed to the nature (and position) of the α-nucleotide. First, the thermostability of these duplexes decreases from the control to alphaC in the following series: control > alphaT ≈ alphaA ≈ alphaG > alphaC. Second, in each of the four α-duplexes, ^{1}H and ^{31}P chemical shift differences compared to those of the control duplex are largely confined to the region encompassing the α-nucleotide and unnatural phosphodiester linkages, as well as neighboring nucleotides. Surprisingly, for alphaC, these modifications result in a significant alteration to the backbone conformation at the phosphodiester group directly across from the 3′−3′ linkage. Finally, spin−spin (*J*) coupling data, specifically Σ1′, indicate that the vast majority of the furanose rings in these duplexes display a high propensity for adopting the S pucker. However, in alphaC, alphaA, and alphaT (but not alphaG), the sugar ring conformation in the nucleotide immediately following the 5′−5′ linkage is described by an approximately equal distribution between the N and S conformers.

Antisense therapy, an enticing approach that is built upon the notion of administering oligodeoxynucleotides (ODNs)[1] to arrest the synthesis of a specific gene product at the level of translation, has led to a large research effort due to its potentially ubiquitous applicability in the treatment of genetically based diseases [recently reviewed by Crooke (1993), Hélène (1994), Wagner (1994), and Lönnberg and Vuorio (1996)]. To optimally function as an antisense agent, it is believed that an ODN must possess a number of important properties, including (1) high resistance to degradation by endogenous nucleases, (2) cellular uptake, (3) highly selective binding to its mRNA target, (4) stable complex formation with its mRNA target (in terms of both T_m and enthalpy), and (5) the RNA strand in the resulting ODN/mRNA hybrid should be sensitive to cleavage by RNase H, destroying the target and liberating the antisense ODN for further mRNA binding/catalysis events. The necessity for cellular longevity resulting from nuclease resistance has stimulated the design of nucleic acids containing a variety of modifications to the phosphodiester backbone (i.e., phosphorothioates and methyl phosphonates), as well as the sugar and base moieties (Milligan et al., 1993; de Mesmaeker et al., 1995a,b).

α-Anomeric nucleotides differ from native β-nucleotides by an inversion of stereochemistry at the C1′ position of the furanose ring. Along with their synthetic feasibility and enantiomeric purity, this single modification confers upon α-ODNs two of the important features listed above that make them potential antisense candidates. (1) α-DNA strands can bind with high affinity to complementary β-DNA and β-RNA strands, potentially forming complexes with stabilities even higher than those of purely β-anomeric controls (Praseuth et al., 1987; Thuong et al., 1987; Paoletti et al., 1989), and (2) α-DNA exhibits high resistance to nuclease degradation (Vichier-Guerre et al., 1994). The structural features of several short α-DNA/β-DNA duplexes were elucidated by NMR spectroscopy, confirming the formation of parallel

† This work was supported in part by a grant from the Natural Sciences and Engineering Research Council of Canada (JHvdS).

* To whom correspondence should be addressed. Telephone: (215) 503-4581. Fax: (215) 923-2117. E-mail: mwg@bern.jci.tju.edu.

‡ Thomas Jefferson University.

§ University of Calgary.

⊗ Abstract published in *Advance ACS Abstracts,* July 15, 1997.

[1] Abbreviations: 1D, one-dimensional; 2D, two-dimensional; DQF-COSY, double-quantum-filtered correlated spectroscopy; DSS, 2,2-dimethylsilapentane-5-sulfonate; DTT, dithiothreitol; ECOSY, exclusive correlation spectroscopy; EDTA, ethylenediaminetetraacetic acid; HPLC, high-performance liquid chromatography; NMR, nuclear magnetic resonance; NOE, nuclear Overhauser enhancement; NOESY, NOE spectroscopy; ODN, oligodeoxynucleotide; PECOSY, primitive ECOSY; TOCSY, total correlated spectroscopy; TPPI, time proportional phase increment; Tris, tris(hydroxymethyl)aminomethane.

S0006-2960(97)00607-7 CCC: $14.00

right-handed duplexes, exhibiting several B-DNA traits, such as Watson−Crick base pairing, anti glycosidic bonds, and primarily S-type sugar puckering (Morvan et al., 1987; Lancelot et al., 1987, 1989; Guesnet et al., 1990; Gmeiner et al., 1992).

However, while α-ODNs have been shown to block mRNA translation *in vitro* and curtail viral growth by alternate mechanisms [i.e., Bertrand et al. (1989), Boiziau et al. (1991), Lavignon et al. (1992), and Zelphati et al. (1994)], purely α-DNA is incapable of eliciting cleavage of complementary *β*-RNA by RNase H. Recently, in an effort to design antisense agents that promote RNase H activity yet retain nuclease resistance and complex stability, α−*β* chimeric ODNs were designed through the use of polarity reversals brought about by 3′−3′ and 5′−5′ phosphodiester linkages (Debart et al., 1994; Koga et al., 1995; van de Sande et al., 1994). Indeed, Boiziau et al. (1995) demonstrated that chimeras containing contiguous α- and *β*-tracts ligated by a 3′−3′ phosphodiester bond and featuring two 5′ ends can arrest reverse transcription via RNase H *in vitro*. Moreover, ODNs containing α-nucleotides, polarity reversals, and RNase H sensitive *β*-windows either flanked by alternating α-*β*-tracts (Germann et al., 1997) or fused to purely α-tracts by pyrophosphate groups (Gottikh et al., 1994) have also been reported.

In light of these developments, there is a need to understand the thermodynamic and underlying structural effects of the combination of α-anomeric nucleotides and polarity reversals, in order to rationally design more potent antisense therapeutics in terms of stability, nuclease resistance, and RNase H sensitivity. In this paper, we provide thermodynamic and spectroscopic data for a set of self-complementary DNA decamers with an identical sequence [5′-d(GCGAATTCGC)-3′], each containing a single α-anomeric nucleotide (αC, αA, or αG) inserted into tracts of *β*-nucleotides by 3′−3′ and 5′−5′ phosphodiester linkages. The results are compared to our previous study on the remaining members of this family, namely the unmodified control and an αT permutation (Aramini et al., 1996). We will demonstrate that all four α-containing decamers form stable, B-like duplexes, with a high degree of structural similarity, although there are subtle thermodynamic and structural differences which are dependent upon the nature of the α-nucleotide.

EXPERIMENTAL PROCEDURES

Synthesis and Purification. The 3′-(dimethoxytrityl)-5′-(2-cyanoethyl *N*,*N*-diisopropylphosphoramidites) of α-D-deoxycytidine, α-D-deoxyadenosine, and α-D-deoxyguanosine were synthesized from their respective nucleosides (R. I. Chemicals Inc.) on the basis of the three-step approach outlined in our earlier work (Aramini et al., 1996). Amidine protection of the amino group was employed in the protocol for α-dG (McBride et al., 1986). Approximately 2−5 *μ*mol (5.5−15 mg) of each decamer [alphaC, d[GCGAATT-3′−3′-(αC)-5′−5′-GC]; alphaA, d[GCG-3′−3′-(αA)-5′−5′-ATTCGC]; and alphaG, d[GC-3′−3′-(αG)-5′−5′-AATTCGC]] was generated using an Applied Biosystems 380B DNA synthesizer, followed by deprotection and purification by gel filtration and HPLC, as we recently described.

5′ End Labeling and Restriction Enzyme Reactions. Oligonucleotides were 5′ end-labeled and purified as previously described (Aramini et al., 1996). End-labeled *Eco*RI substrate, CTACGAATTCGTAG (46.7 pmol), was digested with 5 units of *Eco*RI (Boehringer) in the presence of a 14.8-fold excess of competitor DNA (control, alphaT, alphaC, alphaA, and alphaG decamers) for 30 min at 27 °C in 29 *μ*L of reaction buffer (50 mM Tris, 100 mM NaCl, 10 mM $MgCl_2$, and 1 mM DTT at pH 7.5). The reaction was terminated by heat inactivation, and the products were analyzed by denaturing gel electrophoresis on 15% polyacrylamide gels (8 M urea, 90 mM Tris-borate, and 5 mM EDTA at pH 8.3) and autoradiographed. Bands corresponding to unreacted and digested material were quantified by scintillation counting.

Optical Spectroscopy. Ultraviolet (UV) absorption spectra and thermal denaturation profiles were recorded on a CARY 3E spectrophotometer (Varian) equipped with thermostated cuvette holders. All samples were prepared in 400 mM NaCl, 10 mM Na_2HPO_4, and 0.1 mM EDTA at pH 6.5, and in each case, the strand concentration was calculated from the A_{260} at 85 °C using the molar extinction coefficient for this sequence under denaturing conditions derived from the contributions of the constituent mononucleotides (ϵ_{260} = 104 260 M^{-1} cm^{-1} in 5.0 M $NaClO_4$ at 90 °C and pH 7.2). Hyperchromicity profiles were obtained from 320 → 220 nm scans (100 nm/min, 0.5 nm intervals) at 5 and 85 °C by dividing the absorbance of the denatured form (85 °C) by that of the duplex form (5 °C). The thermal denaturation experiments were performed on samples ranging in total strand concentration from ≈10 to 75 *μ*M; A_{260} readings were recorded at 0.1 °C intervals, and a temperature ramp of 0.4 °C/min was used. Assuming a concerted two-state (helix ↔ coil) process and that the enthalpy is temperature-independent, the enthalpy of formation of the duplex, $\Delta H°$, and the melting temperature, T_m, were extracted from each melting curve (minimum of two curves per concentration) using a six-parameter fitting routine, in which the temperature-dependent absorbances of the helix and coil forms are accounted for (Germann et al., 1988). The entropy ($\Delta S°$) can then be obtained from eq 1, which is valid for self-complementary duplexes:

$$\Delta S° = \frac{\Delta H°}{T_m} - R \ln(C_T) \qquad (1)$$

where R is the gas constant, C_T is the total strand concentration (molar), and the T_m is in kelvin (Breslauer et al., 1996, and references therein). Values of $\Delta H°$ and $\Delta S°$ were also obtained from (van't Hoff) plots of the concentration dependence of $1/T_m$.

NMR Spectroscopy. NMR samples were prepared by dissolving the lyophilized powder in 0.4 mL of 50 mM NaCl, 10 mM Na_2HPO_4, and 0.1 mM EDTA at pH 6.5, containing either a 90% H_2O/10% D_2O mixture (imino ^1H NMR) or D_2O (nonlabile ^1H and ^{31}P NMR).

All NMR experiments were performed on a Bruker AMX 600 NMR spectrometer equipped with a 5 mm broad-band inverse probe, at ^1H and ^{31}P frequencies of 600.1 and 242.9 MHz, respectively, using the XWINNMR 1.1 software package run on a Silicon Graphics INDY workstation. The salient acquisition and processing parameters for the spectra reported here are analogous to those detailed in our earlier work (Aramini et al., 1996) and, briefly, are as follows: (i) 1D 1−1 jump and return imino ^1H NMR (Plateau & Guéron,

1982), 0.8−1.3 s repetition time and 2−5 Hz exponential line broadening; (ii) 1D ^{31}P NMR, ≈45° flip angle, 1.6 s repetition time, zero-filled, and transformed with a line broadening of 1 Hz; (iii) 2D NOESY, 2K data points in t_2, 512 experiments in t_1, 6.7−8.2 s repetition time, presaturation of the residual HDO signal, and TPPI; (iv) 2D ^{31}P−^{1}H correlation (Sklenár et al., 1986), 2K data points in t_2, 400 experiments (5 ppm sweep width) in t_1, 1.3 s repetition time, and TPPI; (v) DQF-COSY{^{31}P}, 4K data points in t_2, 2K experiments in t_1, 2.5 s repetition time, presaturation, ^{31}P decoupling during acquisition, and TPPI; (vi) PECOSY (Mueller, 1987), ≈40° pulse, 4K data points in t_2, 2K experiments in t_1, 1.9 s repetition time, and TPPI; (vii) ECOSY with gradients (Willker et al., 1993), 2.7 s repetition time, 2K data points in t_2, 2K experiments in t_1, and TPPI. All 2D data were processed with 45−90°-shifted sine-bell multiplication in both dimensions. For the purposes of determining spin−spin (*J*) coupling values, DQF-COSY, PE COSY, and ECOSY data were strip transformed, yielding a resolution of 0.6−0.7 Hz/point in both dimensions, and processed using resolution enhancement (i.e., Gaussian multiplication) in an effort to minimize errors due to antiphase peak cancellation. All ^{1}H and ^{31}P NMR spectra were referenced to the absolute frequencies of external DSS and 85% H_3PO_4 in a capillary, respectively, at the appropriate temperature (both in D_2O).

Molecular Modeling. Initial models of the alphaC, alphaA, and alphaG decamer duplexes based on the PDB coordinates of the Dickerson dodecamer (Westhof, 1987) were generated as outlined previously (Aramini et al., 1996). All models were energy minimized with AMMP (Harrison, 1993; Harrison & Weber, 1994) running on a PowerMac 8100 employing the strategy and parameters given in our earlier work, except that a dielectric screen with a 5 Å correlation length was also used.

RESULTS AND DISCUSSION

Rationale and Design. On the basis of modeling (Séquin, 1973) and empirical evidence (*vide supra*), it is well-established that an α-anomeric nucleotide must be in a parallel orientation in order to form a classic Watson-Crick base pair with a complementary β-anomeric (deoxy)ribonucleotide. To acheive this, our approach (Aramini et al., 1996), as well as that of other laboratories (Debart et al., 1994; Koga et al., 1995), is to employ 3′−3′ and 5′−5′ phosphodiester linkages on either end of an α-nucleotide to invert its orientation within the strand. The use of linkage reversals has proven useful in the study of parallel-stranded DNA hairpin motifs (van de Sande et al., 1988; Germann et al., 1995). The DNA duplex family we are interested in here is comprised of a 10-nucleotide, self-complementary sequence, in which the *Eco*RI restriction enzyme site is embedded (Figure 1). The four α-containing decamers consist of one α-nucleotide per strand whose orientation is reversed with respect to the rest of the sequence via 3′−3′ and 5′−5′ phosphodiester bonds. Our goal in this design was to produce a class of antiparallel B-DNA duplexes containing a single α-nucleotide parallel segment and two polarity reversals in each strand, in order to assess the thermodynamic and structural consequences of these perturbations in a systematic fashion. The *Eco*RI recognition sequence situated in the central portion of these duplexes affords an additional means of exploring the structural perturbations caused by the sugar and backbone modifications from the perspective of a sequence specific binding protein.

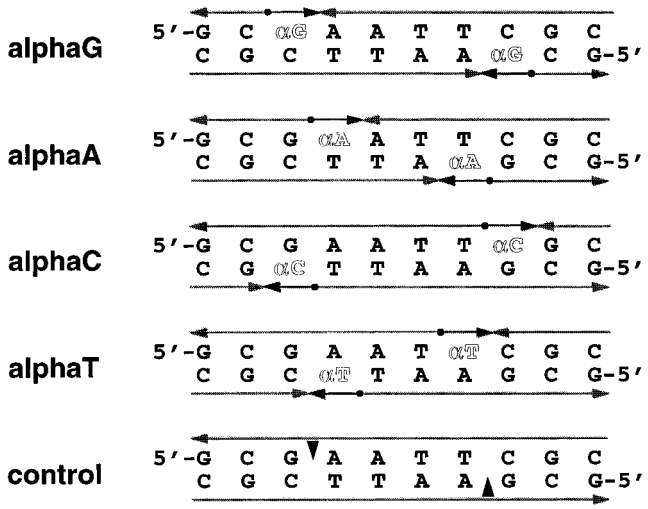

FIGURE 1: Sequences of the family of self-complementary α-containing decamer duplexes relevant to this study and their control. Arrows indicate the strand polarity in the 3′ → 5′ direction; the 3′−3′ and 5′−5′ phosphodiester linkages are denoted by tail-to-tail and head-to-head junctions. α-Anomeric nucleotides are shown in outline type. Black arrows in the control duplex represent the *Eco*RI restriction enzyme cleavage sites.

UV Spectrophotometry. A hyperchromicity profile reflects the increase in the absorbance of ultraviolet light that accompanies the unstacking of bases upon denaturation of duplex DNA and, hence, serves as a sensitive probe for global differences in base stacking and strand disposition among duplexes with the same nucleotide content and sequence (Germann et al., 1988). Hyperchromicity plots of the control sequence as well as the alphaT, alphaC, alphaA, and alphaG decamers are shown in Figure 2A. All five constructs exhibit remarkably similar profiles, especially in terms of the magnitudes and positions of extrema (i.e., maxima at $\lambda \approx 237$ and 278 nm, minimum at $\lambda \approx 260$ nm). Thus, we can conclude that, despite the presence of the modifications, the base pairing and stacking interactions diagnostic of the unmodified decamer duplex have been preserved in the four α-containing sequences.

Thermodynamic Properties of the Duplexes. We have performed thermal denaturation experiments on the alphaC, alphaA, and alphaG decamers in order to compare the thermodynamic consequences arising from the sugar and phosphodiester backbone alterations in each case and, together with the data for the control and alphaT duplexes (Aramini et al., 1996), establish possible links between duplex stability and the nature of the α-nucleotide for this specific sequence. Since our model sequence is self-complementary, particular attention must be given to the potential presence of monomolecular, hairpin structures, as was previously documented for related sequences containing a central *Eco*RI restriction window (Marky et al., 1983; Rinkel et al., 1987b). The near identical hyperchromicity profiles of the five decamers shown above suggest no hairpin formation at low temperature, high salt (400 mM NaCl), and low oligonucleotide concentration; this was confirmed by imino ^{1}H NMR spectra obtained at UV concentrations (*vide infra*). However, in the case of alphaT, we demonstrated that the introduction of unnatural moieties in the central

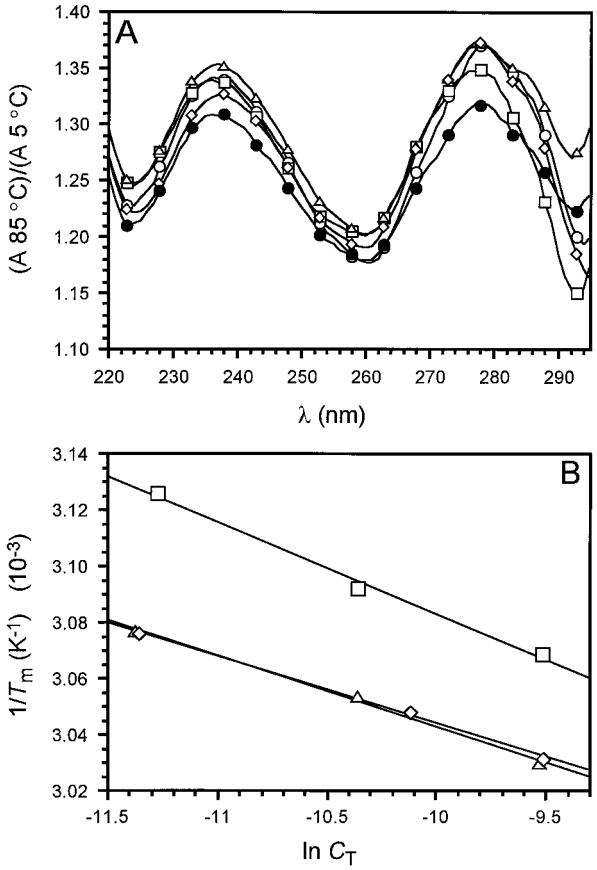

FIGURE 2: (A) Hyperchromicity profiles of (●) 8.0 μM control duplex, (○) 7.4 μM alphaT duplex, (□) 7.7 μM alphaC duplex, (△) 7.5 μM alphaA duplex, and (◇) 7.6 μM alphaG duplex recorded in 400 mM NaCl, 10 mM Na_2HPO_4, and 0.1 mM EDTA at pH 6.5. Markers indicate every fifth point. (B) Concentration dependence of the T_m for the alphaC (□), alphaA (△), and alphaG (◇) duplexes; C_T represents the total strand concentration.

region of the sequence (i.e., αT7) stabilizes the hairpin form relative to the dimer species at elevated temperatures (Aramini et al., 1996). For the alphaC, alphaA, and alphaG decamers, we observe no change in enthalpy over the concentration range examined (≈10−75 μM), as well as linear van't Hoff plots (Figure 2B). Thus, we can conclude that in each case a purely two-state (helix ↔ coil) transition is occurring without interference from a hairpin intermediate under these conditions; this is expected for the alphaC and alphaG decamers, where the modifications are situated in the stem portion of the putative hairpin, thereby destabilizing this form with respect to the dimer. Thermodynamic data (i.e., T_m at a C_T of 30 μM, $\Delta H°$, and $\Delta S°$) for the alphaC, alphaA, and alphaG decamers, as well as for the control and alphaT sequences (Aramini et al., 1996), are listed in Table 1. From the T_m and $\Delta H°$ values, we note that the alphaC duplex is markedly less stable than the others in this family, and the following thermostability series is observed for these duplexes (highest → lowest): control > alphaT ≈ alphaG ≈ alphaA > alphaC. Very recent studies in our laboratories on a variant of the alphaT sequence that contains exclusively 3′-5′ phosphodiester bonds revealed that the polarity reversals are absolutely essential for stable duplex formation (J. M. Aramini and M. W. Germann, unpublished results). This rule, however, does not hold for chimeric DNA duplexes containing other types of sugar modifications (i.e., L-nucleosides) (Dahma et al., 1994).

Table 1: Thermodynamic Data for the Control and α-Containing Decamer Duplexes[a]

duplex	T_m (°C)	$\Delta H°$ (kJ mol^{-1})	$\Delta S°$ (kJ mol^{-1} K^{-1})
control[b]	59.8 (0.1)	343 (12)	0.940 (0.033)
alphaT[b]	54.7 (0.3)	330 (15)	0.946 (0.021)
alphaC	49.8 (0.3)	258 (7)	0.712 (0.022)
alphaA	54.4 (0.2)	323 (13)	0.898 (0.041)
alphaG	54.3 (0.3)	334 (14)	0.933 (0.043)

[a] All measurements were performed under the following buffer conditions: 400 mM NaCl, 10 mM Na_2HPO_4, and 0.1 mM EDTA at pH 6.5. The melting temperatures reported were calculated for a C_T of 30 μM on the basis of the $1/T_m$ vs ln(C_T) curves shown in Figure 2B. The $\Delta H°$ and $\Delta S°$ values reported are weighted averages of the results from the fits at each individual concentration and the slope ($m = R/\Delta H°$) and *y*-intercept ($b = \Delta S°/\Delta H°$), respectively, of the van't Hoff plots. Standard deviations are given in parentheses. [b] Data obtained from Aramini et al. (1996).

Interestingly, the distinctly lower stability observed for alphaC contrasts with earlier thermodynamic studies of DNA duplexes containing purely α- and β-anomeric strands, in which it was found that α-pyrimidines conferred greater thermodynamic stability than α-purines (Paoletti et al., 1989); Debart et al. (1994) also showed that the stabilities of complexes involving fully alternating α−β chimeric DNA sequences decreased with increasing α-purine content. However, comparisons to our model system, which differs from these examples in terms of sequence (i.e., β-stretches flanking a single α-nucleotide) and structure, should be made with caution.

EcoRI Digestions. The family of DNA decamers studied here contains an *Eco*RI recognition sequence, in which the phosphodiester linkages between G3 and A4 in each strand are cleaved by the enzyme (Figure 1). Hence, our model system features a built-in biochemical assay for changes in the structural integrity of the duplex due to the introduction of α-anomeric nucleotides and unnatural phosphodiester bonds. This strategy has been successful in demonstrating loop-induced perturbations to the stem structure in hairpins (Germann et al., 1990).

We have reported that alphaT is completely resistant to hydrolysis by *Eco*RI (Aramini et al., 1996); not surprisingly, we now find that alphaC, alphaA, and alphaG are also not substrates for this enzyme. However, this does not rule out the possibility that these species can bind to the enzyme without being cleaved. For all α-duplexes investigated here, the base pair determinants in the major (and minor) groove are indistinguishable from those in the control (see Model of the α-Duplex Decamer below). This leads us to predict that *Eco*RI should still be able to form the network of hydrogen bonds and van der Waals contacts that have been reported for the complex [for a review, see Heitman (1992)]. In order to assess this, we have conducted *Eco*RI inhibition assays, in which an *Eco*RI substrate (CTACGAATTCGTAG) is digested in the presence of a decamer. The 14-mer was chosen rather than the control decamer to avoid unwanted heteroduplex formation, which would hinder the interpretation of the results. Under these conditions, we find that, while a hairpin control lacking the *Eco*RI consensus sequence does not decrease the digestion of the 14-mer, the control, alphaT, alphaC, alphaA, and, to a lesser extent, alphaG decamers do (Table 2). From this competition assay, we can conclude that the four α-decamers can bind to the restriction enzyme, while the control hairpin does not. In

Table 2: *Eco*RI Digestions of CTACGAATTCGTAG in the Presence of Various inhibitors[a]

inhibitor	% digestion
none	42
control decamer	14
alphaT decamer	24
alphaC decamer	24
alphaA decamer	25
alphaG decamer	38
control hairpin	41

[a] Inhibitors were added in a 14.8-fold excess; comparable results were obtained under conditions where less material was digested. The control hairpin GCGAGCTAGCGTTTCGCTAGCTCGC does not contain the *Eco*RI consensus sequence and does not act as an inhibitor.

the case of alphaG, in which the scissile GpA bonds are replaced by 5′−5′ phosphodiester linkages, the affinity is significantly lower compared to that of the alphaT and alphaC, as well as that of the alphaA decamer in which 3′−3′ linkages constitute the sites of cleavage. It has been established that DNA bound specifically by this enzyme is significantly distorted (Heitman, 1992); moreover, the energetics of the *Eco*RI−DNA interaction are affected by the sequences flanking the recognition module. Thus, it is conceivable that the lower affinity exhibited by alphaG, and to a smaller extent alphaC, alphaA, and alphaT, originates from such effects.

NMR Spectroscopy. Base Pairing and Imino ^{1}H NMR. The unique intrinsic chemical shifts of imino protons ($\delta \approx 10-15$ ppm) make them extremely useful direct monitors of base pairing in nucleic acids. Imino ^{1}H NMR spectra of the control and the four α-containing decamers are shown in Figure 3; the assignments shown were obtained from the imino-imino proton NOE contacts between consecutive base pairs [i.e., d_{ps}(G1,1;G9,1) through to d_{ps}(T7,3;T6,3)] using the 1−1 NOESY technique (Sklenár & Bax, 1987a; not shown).[2] In each case, one observes five distinct imino ^{1}H signals, the number expected for a self-complementary decamer duplex. Although there are subtle differences in the positions of the T imino protons across the series, as well as the upfield shift of the αG3 imino proton in the alphaG duplex, the imino ^{1}H NMR data provide strong evidence in favor of the formation of stable base pairing and stacking in all five duplexes. In each case, imino proton spectra recorded at increasing temperatures did not indicate any premelting behavior of the base pairs containing the α-nucleotides. Near identical resonance patterns are detected at micromolar concentrations of the alphaC, alphaA, alphaG (inset of Figure 3), and alphaT (Aramini et al., 1996) decamers, conclusively demonstrating duplex formation and indicating that the structural traits of these duplexes are preserved in the conditions used for the optical studies described above.

^{1}H NMR Assignments and NOESY Walks. The signals corresponding to the nonlabile protons in the alphaC, alphaA, and alphaG duplexes were assigned by standard through-space (i.e., NOESY) and through-bond (COSY-type experiments, TOCSY, and ^{31}P−^{1}H correlation) techniques (Wüthrich, 1986). All ^{1}H (and ^{31}P) assignments for these duplexes are available as Supporting Information. In this section, we summarize a number of spectroscopic properties consistent with an overall right-handed helical B-DNA structure in these duplexes.

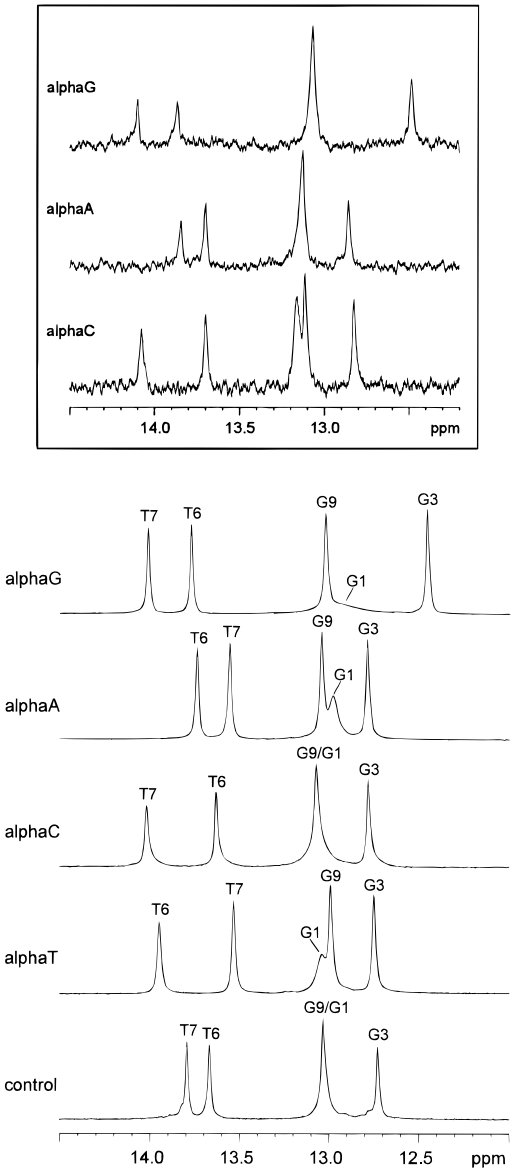

FIGURE 3: Imino proton region of the ^{1}H (600.1 MHz) NMR spectra of the control duplex (2.6 mM), alphaT duplex (6.8 mM), alphaC duplex (2.4 mM), alphaA duplex (2.9 mM), and alphaG duplex (2.2 mM) in 50 mM NaCl, 10 mM Na_2HPO_4, and 0.1 mM EDTA at pH 6.5 and 293 K. (Inset) imino ^{1}H (600.1 MHz) spectra of the alphaC, alphaA, and alphaG decamers recorded at optical concentrations (≈3−6 μM duplex concentration, same buffer as above except 400 mM NaCl was used, 280−283 K, 10K scans each).

First, for the alphaC, alphaA, and alphaG decamers we observe a break in the H2′/H2″−base NOE connectivity pathway [i.e., d_i(6,8;2′) → d_s(2″;6,8)] diagnostic of right-handed B-DNA, between the H2″ (and H2′) of the α-nucleotide and the base proton of the subsequent residue in the sequence (Figure 4). However, the analogous H1′−base network [i.e., d_i(6,8;1′) → d_s(1′;6,8)] remains intact; in fact, we consistently detect a rather intense sequential contact between the H1′ of the α-nucleotide and the H6/H8 of the

[2] The short-hand used in this paper to represent NOE contacts between two protons follows the convention given by Wüthrich (1986); i.e., for two nuclei A and B, d_i(A;B) denotes an intranucleotide distance; d_s(A;B) represents a sequential (same strand) contact between nonlabile protons, where A and B are in the 5′ and 3′ nucleotides, respectively; d_{pi}(A;B) symbolizes an interstrand distance between protons (including A H2) within a base pair; and d_{ps}(A;B) defines a contact between labile protons in juxtaposed base pairs.

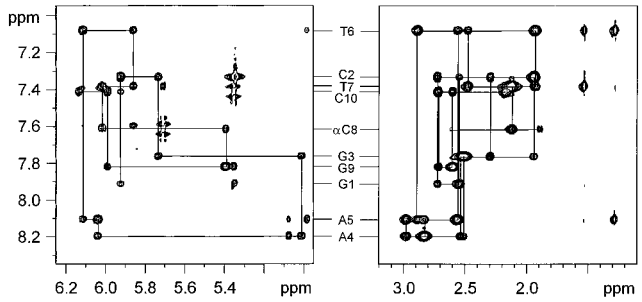

FIGURE 4: NOESY ($\tau_m = 75$ ms) spectrum of alphaC (5.9 mM) in D_2O at 303 K. (Left) H6/8(ω_1)−H1′(ω_2) region. (Right) H6/H8-(ω_1)−H2′/H2″(ω_2) region.

ensuing nucleotide. We have previously noted these phe nomena for the alphaT decamer of this series (Aramini et al., 1996) and attribute them to a change in the orientation of the furanose ring for the α-nucleotide compared to the other residues in the sequence (see Modeling of the α-Duplex Decamer below).

Second, we observe that significant nonlabile ^{1}H chemical shift differences between the α-duplexes and the control are generally restricted to the α-nucleotide and, occasionally, nucleotides flanking it or complementary to it. For each α-nucleotide, the H2′ signal is significantly downfield of its geminal partner, H2″, which is opposite to what is commonly observed in B-DNA; the H4′ resonance also displays a large downfield shift in all the α-sugars compared to the β-anomers (Lancelot et al., 1987). In addition, we observe the coalescence or even reversal of the geminal H2′/H2″ resonance positions for the nucleotide preceding the α-nucleotide in each case (i.e., T7 in alphaC, C2 in alphaG, and G3 in alphaA), as well as marked changes in the chemical shifts of several sugar protons (i.e., H1′, H2′, and H2″) in the guanosine opposite the α-nucleotide in alphaC.

Several other NOE contacts diagnostic of B-DNA are preserved in the α-duplexes. From the much closer proximity of the H6/H8 and H2′/H2″ protons compared to that of the H1′ protons, we can conclude that all bases in these duplexes are in the anti conformation with respect to the furanose ring [i.e., d_i(6,8;2′,2″) < d_i(6,8;1′)]. Concerning the α-nucleotides, this is further substantiated by a relatively intense d_i(6,8;4′) cross-peak for each α-anomeric sugar (Lancelot et al., 1987; Gmeiner et al., 1992). Furthermore, we observe the established sequential NOE contacts between protons in the major groove, d_s(6,8;M), and minor groove, d_s(2;2), as well as intra-base pair connectivities, d_{pi}(T3;A2), consistent with Watson−Crick base pairing and normal double-helical B-DNA. Finally, the isolated H2 adenine base protons possess exceedingly long longitudinal (T_1) values in D_2O at 303 K (alphaA A4, 4.2 s; alphaA A5, 4.0 s; alphaG A4, 5.4 s; and alphaA A5, 5.3 s),[3] reflecting their location in a proton poor minor groove.

Taken together, the numerous trends and properties outlined above provide strong evidence that each of the three α-decamers adopts overall antiparallel B-DNA duplexes, with any notable spectroscopic perturbations confined to the regions encompassing the α-nucleotides and unorthodox

[3] The T_1 values were determined by the inversion-recovery method; spectral overlap in the base region of the ^{1}H NMR spectrum precluded the T_1 determinations for the two adenine H2s in alphaC.

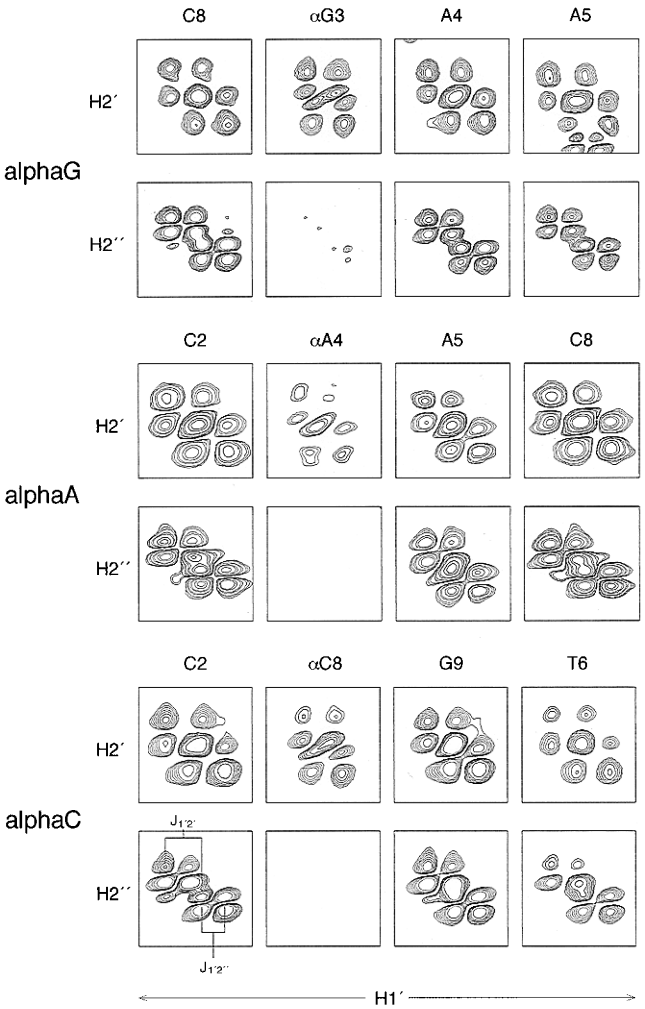

FIGURE 5: Expansions (60 Hz in ω_1 x 30 Hz in ω_2) of the H2′ and H2″(ω_1)/H1′(ω_2) PECOSY (alphaC and alphaG) and ECOSY (alphaA) cross-peaks of selected nucleotides in these decamers. In each case, we show the multiplet patterns for two normal, high-S-pucker sugars (outside pair), along with the fine structure for the α-anomeric sugars and the nucleotide following the 5′−5′ linkage in the sequence. The extraction of individual coupling constants on the basis of active and passive couplings is displayed for the H2″−H1′ multiplet of C2 in alphaC. Positive contours are displayed in red and negative contours in black.

phosphodiester linkages, as we recently demonstrated for the alphaT construct (Aramini et al., 1996).

Sugar Ring Puckering. A number of investigations have demonstrated that the conformation, or puckering, of a furanose ring within a nucleic acid can be elucidated by knowledge of the spin−spin coupling constants between neighboring furanose ring protons, in particular H1′ through H3′ [recently reviewed by Wijmenga et al. (1993) and van Wijk et al. (1992)]. For deoxyribose sugars in the limit of rapid conformational exchange between two states, the N (C3′-endo) and S (C2′-endo) puckers, any intraresidue coupling constant one measures, J_{XY}, is simply a linear combination of the product of that coupling constant in the purely N and S pucker and its respective mole fraction, f_N or f_S (eq 2).

$$J_{XY\,\mathrm{obs}} = f_N J^N_{XY} + f_S J^S_{XY} \qquad (2)$$

The Altona group has shown that one can employ the sum of the H1′ coupling constants (Σ1′) to obtain a snapshot of

Table 3: Sugar Puckering Data for the Control and α-Containing Decamer Duplexes[a]

	control		alphaT		alphaC		alphaA		alphaG	
Nt	Σ1′	f_s	Σ1′	f_s	Σ1′	f_s	Σ1′	f_s	Σ1′	f_s
G1	15.2	0.92	15.3	0.93	14.6	0.81	14.3	0.76	14.9	0.86
C2	15.1	0.90	14.7	0.83	15.0	0.88	15.0	0.88	(15.3)	(0.93)
G3	16.2	1.00	15.9	1.00	14.9	0.86	16.0	1.00	*9.4*	–
A4	16.2	1.00	15.3	0.93	15.3	0.93	*10.7*	–	**14.5**	**0.80**
A5	15.7	1.00	15.3	0.93	15.1	0.90	**12.1**	**0.39**	14.9	0.86
T6	15.1	0.90	15.3	0.93	14.7	0.83	14.6	0.81	14.8	0.84
T7	16.0	1.00	*12.3*	–	(15.3)	(0.93)	15.0	0.88	15.6	0.98
C8	15.1	0.90	**12.9**	**0.53**	*9.5*	–	15.0	0.88	14.4	0.82
G9	15.7	1.00	14.7	0.83	**13.5**	**0.63**	14.3	0.76	14.9	0.86
C10	(14)	(0.7)	(14)	(0.7)	(14)	(0.7)	(14)	(0.7)	(14)	(0.7)

[a] Data obtained from (i) the H2″(ω_1)/H1′(ω_2) multiplets along ω_2 in a resolution-enhanced DQF-COSY spectrum (control and alphaT) and (ii) the H2″(ω_1)−H1′(ω_2) multiplets in a resolution-enhanced PECOSY (alphaC and alphaG) or ECOSY (alphaA). Data for α-sugars and sugars in the nucleotide bound to the 5′−5′ phosphodiester linkage are shown in italics and boldface, respectively. In cases where the H2′ and H2″ resonances are markedly overlapped, we resorted to the DQF-COSY (outer most peaks of multiplets) to extract the Σ1′ data (given in parentheses). The mole fraction of S pucker (f_s) for each sugar was calculated from the Σ1′ using eq 3 (see the text).

the fraction of a given nucleotide whose sugars adopt an S pucker (eq 3; Rinkel & Altona, 1987).[4]

$$f_s = \frac{\Sigma 1' - 9.8}{5.9} \qquad (3)$$

We have used DQF-COSY and ECOSY-type experiments, of which the latter give rise to simpler multiplet patterns (i.e., Figure 5), to obtain Σ1′ values for the sugar moieties in each of the five duplexes via the H2″ or H2′ ↔ H1′ multiplet patterns; these data are listed in Table 3. Ignoring the 3′-terminal nucleotide, the corresponding Σ1′ values for virtually all the β-anomeric sugars in each duplex are indicative of a strong preference for the S pucker (i.e., Σ1′ > 14 Hz). This notion is further supported by the observation that $^3J_{1'2'}$ is consistently larger than $^3J_{1'2''}$, as well as the weak or completely absent $^3J_{2''3'}$ (not shown), which are highly diagnostic of S puckering. These data are consistent with the large body of *J* coupling evidence pertaining to the conformational traits of deoxyribose rings in natural B-DNA duplexes, such as the self-complementary decamer d(CCGAATTCGG)$_2$ ($f_S \approx$ 70 to 100%; Rinkel et al., 1987a).

There are, however, exceptions to this trend. In three of the α-containing duplexes (alphaT, alphaC, and alphaA), the β-sugar in the nucleotide juxtaposed with respect to the 5′−5′ phosphodiester linkage is shifted significantly toward the N pucker. Again, the Σ1′ data are corroborated by the magnitudes of the individual H1′ coupling constants (i.e., $^3J_{1'2'} \leq {}^3J_{1'2''}$) and the presence of an H2″−H3′ cross-peak (not shown). All α-anomeric sugars in these duplexes exhibit rather unusual properties, namely low Σ1′, but $^3J_{1'2'} \gg {}^3J_{1'2''}$, and no $^3J_{2''3'}$. This is thought to reflect a preference for the S-type conformer, albeit with a reduced puckering amplitude (Gmeiner et al., 1992).

Backbone Conformation and ^{31}P NMR. It is widely accepted that the ^{31}P chemical shift is highly dependent on factors that govern the conformation of the phosphodiester backbone (i.e., phosphate ester torsional angles and helical parameters), making ^{31}P NMR spectroscopy a sensitive and convenient probe for the dynamic and structural properties of sugar−phosphate backbones in nucleic acids and their complexes [for a recent review, see Gorenstein (1994)]. ^{31}P NMR spectra for the control, alphaT, alphaC, alphaA, and alphaG duplexes are shown in Figure 6. In each case, we observe the expected nine ^{31}P resonances, whose assignments are facilitated by ^{31}P−^{1}H correlation spectroscopy (Sklenár et al., 1986); the spectrum for alphaC is shown in Figure 7. Notice that for each of the four α-containing duplexes one observes two signals markedly shifted from the cluster found for the B-DNA control duplex at $\delta \approx -0.3$ to -0.8 ppm. On the basis of correlations to either only H3′ or H5′/H5″ (Figure 7), we assign the upfield ($\delta \approx -1.6$ to -2.2 ppm)- and downfield ($\delta \approx 0.7-1.2$ ppm)-shifted ^{31}P signals in these decamers to the 3′−3′ and 5′−5′ phosphodiester linkages, respectively [see also Germann et al. (1989) and Koga et al. (1995)]. In general, the resonances corresponding to the remaining seven phosphorus atoms in the α-sequences also

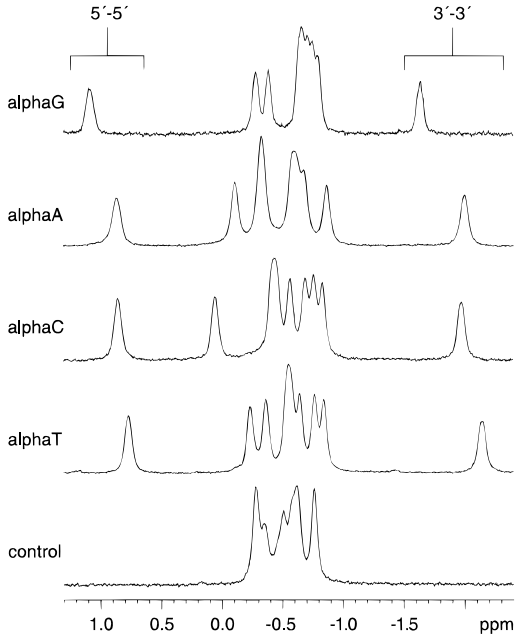

FIGURE 6: ^{31}P (242.9 MHz) NMR spectra of the control (2.6 mM), alphaT (6.8 mM), alphaC (5.9 mM), alphaA (5.1 mM), and alphaG (2.2 mM) duplexes in D_2O at 303 K.

[4] Equation 3 was derived from eq 2 using the calculated values of $J^N_{1'2'}$, $J^N_{1'2''}$, $J^S_{1'2'}$, and $J^S_{1'2''}$ corresponding to the following assumed pseudorotation angles, *P*, and puckering amplitudes, Φ, for the pure N and S states: $P_N = 9°$, $\Phi_N = 35°$; and $P_S = 156°$, $\Phi_S = 35°$ (Rinkel & Altona, 1987). The empirical sum of the H1′ coupling constants (Σ1′) is thought to be a good reflection of f_S due to its lack of sensitivity to fluctuations in P_S and Φ_S, when the S conformer is favored (van Wijk et al., 1992).

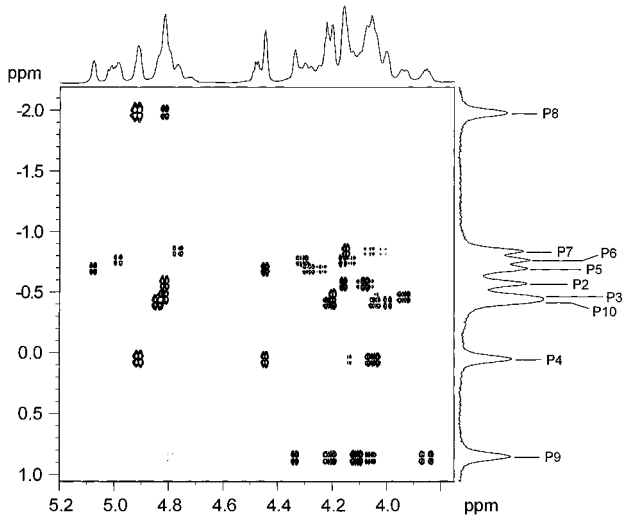

FIGURE 7: ^{1}H-detected ^{31}P−^{1}H correlation spectrum of the alphaC duplex (5.9 mM) in D_2O at 303 K. Coincidental 1D ^{1}H and ^{31}P spectra are shown along the ω_2 and ω_1 dimensions, respectively. Assignments for each of the nine chemically distinct phosphorus atoms in the molecule (where P2 = G1-P-C2, P3 = C2-P-G3, etc.) are also given. Notice that the H3′(βT7)−P8 and H3′(αC8)−P8 cross-peak intensities are markedly different, suggesting an altered backbone conformation about this linkage. The relaxation properties (i.e., chemical shift anisotropy) of ^{31}P at this field strength preclude the quantitative determination of the respective coupling constants using the selective variant of this pulse program, as previously noted (Sklenár & Bax, 1987b).

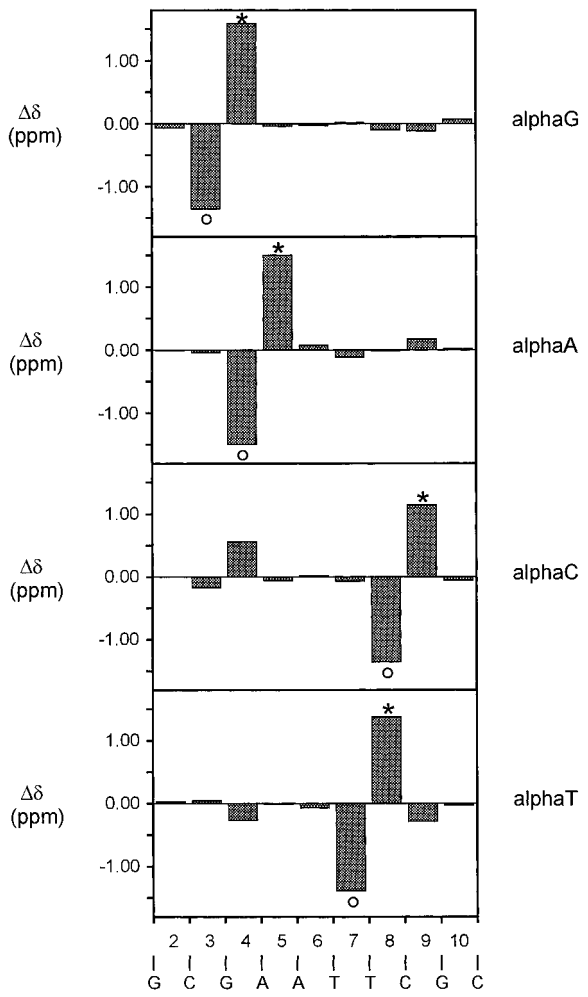

FIGURE 8: Bar graph showing the change in the ^{31}P chemical shift ($\Delta\delta^{31}$P) between the α-containing duplexes and the control for each phosphorus atom in the sequence. Positive and negative values represent downfield and upfield shifts, respectively, in peak position with respect to the control.

fall in the narrow B-DNA window. One major exception to this trend is the signal due to P4 of alphaC (i.e., G3pA4), which is located directly across from the 3′−3′ linkage, in the complementary strand. This is depicted graphically in Figure 8, which shows the change in the ^{31}P chemical shift for the phosphorus atoms in each of the α-duplexes compared to that for the corresponding phosphorus in the unmodified control. Since the sequence is identical for the entire family, these shift differences eliminate any positional and sequence specific effects on the ^{31}P shift and purely reflect the perturbations at each phosphodiester moiety in the backbone in going from the control to each α-decamer. Again, the unusual 3′−3′ and 5′−5′ linkages cause huge upfield and downfield shifts that are remarkably similar in magnitude across the series (3′−3′, $\Delta\delta^{31}$P ≈ −1.4 to −1.5; 5′−5′, $\Delta\delta^{31}$P ≈ +1.1 to +1.5 ppm). While the majority of the other signals display relatively minor chemical shift changes, the peak for P4 of alphaC moves dramatically (≈0.6 ppm) downfield from its resonance position in the control. Significant (≈0.6−2 ppm) downfield ^{31}P shifts have been reported, for example, in B-DNA duplexes containing single mismatches and attributed to a shuffling in the relative populations of the B_{II} [α, β, ϵ, and ζ, gauche(−), trans, gauche(−), trans] and the energetically preferred B_I [α, β, ϵ, and ζ, gauche(−), trans, trans, and gauche(−)] conformations, toward B_{II} [i.e., Roongta et al. (1990) and Chou et al. (1992)]. Moreover, in a recent study of a stable, fully Watson−Crick base-paired DNA duplex containing an unnatural L-nucleoside, conformational changes were reported for the phosphodiester groups linking the L-nucleoside to neighboring D-residues and are manifested by 0.6−1.0 ppm shifts in the corresponding ^{31}P signals (Blommers et al., 1994). While we have yet to confirm this using torsional angle data (i.e., ϵ and ζ via $^{3}J_{H3'-P}$), the backbone conformation in the region of the alphaC duplex encompassing the unnatural phosphodiester linkages is clearly perturbed. Our spectroscopic data do, albeit, provide some structural basis for the significant drop in the thermodynamic stability displayed by this duplex compared to that of the others in this family.

Model of the α*-Duplex Decamer*. Portions of the control, alphaC, alphaA, and alphaG AMMP models encompassing the α-anomeric nucleotides are shown in Figure 9. Note that, for each of the models discussed in this section, NMR (NOE and coupling constant) restraints were not incorporated into the calculations. The models suggest that structural perturbations between the three α-containing duplexes and the control are localized to the α-nucleotide and the unusual backbone linkages (Table 4). Specifically, within each α-nucleotide, the major differences originate in the sugar moiety, whose orientation is completely reversed compared to the surrounding β-nucleotides, whereas the base pairing and stacking interactions are largely preserved. Thus, the combination of the inversion of stereochemistry at C1′ and the polarity reversal facilitates normal Watson−Crick base pairing and stacking for the α-nucleotides at the expense of modifications to the sugar−phosphate backbone. These conclusions are consistent with both the hyperchromicity and NMR data presented above. Moreover, in each of the

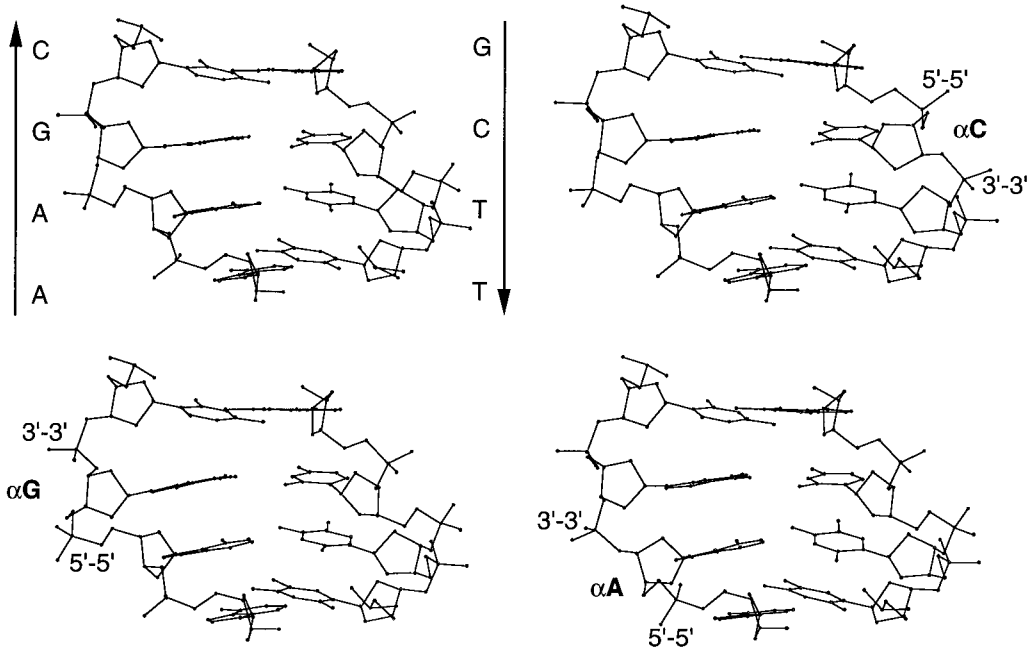

FIGURE 9: Models of control and alphaC, alphaG, and alphaA decamers generated using AMMP as outlined in Experimental Procedures. In each case, only the 5′-CGAA portion encompassing the α-anomeric nucleotides is shown. Strand polarity is represented by arrows. The locations of the α-anomeric nucleotides as well as the 5′−5′ and 3′−3′ linkages are indicated.

Table 4: Properties of the Minimized Model Structures of the Control, AlphaT, AlphaC, AlphaA, and AlphaG Duplexes[a]

parameter	control	alphaT	alphaC	alphaA	alphaG
E (kJ mol^{-1})	−12 461	−12 394	−12 440	−12 419	−12 423
rmsf (kJ mol^{-1} Å^{-1})	3.2	1.6	1.5	2.4	2.4
maxf (kJ mol^{-1} Å^{-1})	11.0	10.0	6.7	12.6	15.9
rmsd (Å)	−	0.30	0.30	0.32	0.30

[a] E, total potential energy (bond, angle, torsion, hybrid, and nonbonded); rmsf, root mean square force; maxf, maximal force; rmsd, root mean square deviation of heavy atoms for the α-decamers from the control (excluding α-anomeric residues and their counterpart in the control, in each case).

α-models, the β-nucleotides are in the anti conformation, whereas the α-nucleotides exhibit positive values for χ (≈109−147°) which roughly fall in the high anti range, after one applies a −200° correction (Lancelot et al., 1989). In addition, the diagnostic sequential distances, d_s(2″;6,8) and d_s(1′;6,8), in all models are consistent with our spectroscopic results. (1) The H1′−base NOE pathway remains intact through the α-nucleotide. (2) The H1′ of the α-nucleotide is in general significantly closer to the H6/H8 of the subsequent nucleotide compared to a typical β-nucleotide. (3) The flip in the orientation of the sugar ring α-nucleotides places the H2″ too far away from the H6/H8 of the next nucleotide (>5 Å), accounting for the break in the H2′/H2″−base NOE pathway at this point. Moreover, each of the α-models predicts short sequential contact between the H1′ of the α-1 residue and the H2″ of the α-nucleotide, which we confirmed upon reinspection of the NOESY data for all four duplexes. However, our models do not account for either the predicted perturbation of the phosphodiester backbone for GpA across from the 3′−3′ linkage in alphaC or the alteration of the puckering in the sugar ring of the β-nucleotide juxtaposed with respect to the 5′−5′ linkage in alphaC and alphaA (as well as alphaT; Aramini et al., 1996). Hence, in order to elucidate the structural details of these duplexes, particularly in the vicinity of the unnatural moieties, we are in the process of calculating high-quality NMR structures via full relaxation matrix approaches (Borgias & James, 1990) combined with homo- and heteronuclear coupling constant information [i.e., Sklenár and Bax (1987b) and Schmieder et al. (1992)].

CONCLUSIONS

In light of the recent interest in the development of chimeric oligonucleotides consisting of an assortment of α- and β-nucleotides linked together by unusual phosphodiester linkages, it is important to gain insights into the thermodynamic and structural effects of such moieties in order to rationally design more effective antisense drugs that are capable of eliciting RNase H activity, while maintaining a high affinity for their specific RNA target and high nuclease resistance. In this paper, we have conclusively demonstrated that native β-anomeric DNA sequences containing any single α-anomeric nucleotide inserted into the strand in the opposite direction via 3′−3′ and 5′−5′ phosphodiester linkages can form stable duplexes whose structures emulate canonical B-DNA. Of the four α-containing sequences, alphaT, alphaA, and alphaG approach the control in terms of stability, and all four exhibit structural perturbations proximal to and encompassing the α-nucleotide and polarity reversals. Moreover, depending on the nature of the α-nucleotide, we found subtle differences in the thermodynamic and structural properties across the family of sequences examined, with the most deleterious effects observed in the alphaC case.

However, caution should be exercised in extrapolating our results to ODNs containing α-anomeric nucleotides within a different sequence context. Also, in the duplexes investigated here, the two isolated α-anomeric nucleotides are each flanked by 3′−3′ and 5′−5′ phosphodiester linkages, whereas in a realistic antisense design, only one or two polarity reversals are required and an extended stretch of α-anomeric nucleotides is preferable on the basis of the stabilities of α-ODN/DNA and α-ODN/RNA duplexes.

On the basis of our results on this model system, we are currently investigating means of alleviating the stress caused by the 3′−3′ linkage, as well as extending our methodology to the investigation of the interactions of analogous α-containing DNA strands with complementary RNA targets. By systematically altering the nature of the polarity-reversed α-anomeric nucleotide within this *β*-sequence, we have gained insight into the thermodynamic and underlying structural consequences of the presence of α-anomers for each of the four common deoxyribose nucleotides and flanking 3′−3′ and 5′−5′ phosphodiester linkages, thereby illustrating the importance of carefully considering both nucleotide content and sequence location of such moieties in the rational design of future, more potent antisense molecules.

ACKNOWLEDGMENT

We are indebted to Mr. Bernd W. Kalisch (University of Calgary) for conducting the *Eco*RI experiments and Dr. Richard T. Pon (University of Calgary) for synthesizing and purifying the oligonucleotides used in this study. We also thank Dr. Eric Wickstrom (Thomas Jefferson University) for access to his CARY UV spectrophotometer and Dr. Robert Harrison (Thomas Jefferson University) for assistance in the modeling studies using his AMMP program.

SUPPORTING INFORMATION AVAILABLE

A table of ^{1}H and ^{31}P resonance assignments for alphaC, alphaA, and alphaG decamer duplexes; portions of the NOESY (τ_m = 75 ms) spectra of alphaA and alphaG (analogous to Figure 4); $^{31}P-^{1}H$ correlation spectra of alphaA and alphaG (analogous to Figure 7); and the H2′/H2″(ω_1)−H1′/H3′(ω_2) region of the DQF-COSY{^{31}P} spectra of alphaC, alphaA, and alphaG (10 pages). Ordering information is given on any current masthead page.

REFERENCES

Aramini, J. M., Kalisch, B. W., Pon, R. T., van de Sande, J. H., & Germann, M. W. (1996) *Biochemistry 35*, 9355−9365.
Bertrand, J. R., Imbach, J.-L., Paoletti, C., & Malvy, C. (1989) *Biochem. Biophys. Res. Commun. 164*, 311−318.
Blommers, M. J. J., Tondelli, L., & Garbesi, A. (1994) *Biochemistry 33*, 7886−7896.
Boiziau, C., Kurfurst, R., Cazenave, C., Roig, V., Thuong, N. T., & Toulmé, J.-J. (1991) *Nucleic Acids Res. 19*, 1113−1119.
Boiziau, C., Debart, F., Rayner, B., Imbach, J.-L., & Toulmé, J.-J. (1995) *FEBS Lett. 361*, 41−45.
Borgias, B. A., & James, T. L. (1990) *J. Magn. Reson. 87*, 475−487.
Breslauer, K. J. (1996) *Methods Enzymol. 259*, 221−243.
Chou, S.-H., Cheng, J.-W., Fedoroff, O. Y., Chuprina, V. P., & Reid, B. R. (1992) *J. Am. Chem. Soc. 114*, 3114−3115.
Crooke, S. T. (1993) *FASEB J. 7*, 533−539.
Dahma, M. J., Giannaris, P. A., & Marfey, P. (1994) *Biochemistry 33*, 7877−7885.
De Mesmaeker, A., Häner, R., Martin, P., & Moser, H. E. (1995a) *Acc. Chem. Res. 28*, 366−374.
De Mesmaeker, A., Altmann, K.-H., Waldner, A., & Wendeborn, S. (1995b) *Curr. Opin. Struct. Biol. 5*, 343−355.
Debart, F., Tosquellas, G., Rayner, B., & Imbach, J.-L. (1994) *Bioorg. Med. Chem. Lett. 4*, 1041−1046.
Germann, M. W., Kalisch, B. W., & van de Sande, J. H. (1988) *Biochemistry 27*, 8302−8306.
Germann, M. W., Vogel, H. J., Pon, R. T., & van de Sande, J. H. (1989) *Biochemistry 28*, 6220−6228.
Germann, M. W., Kalisch, B. W., Lundberg, P., Vogel, H. J., & van de Sande, J. H. (1990) *Nucleic Acids Res. 18*, 1489−1498.
Germann, M. W., Zhou, N., van de Sande, J. H., & Vogel, H. J. (1995) *Methods Enzymol. 261*, 207−225.
Germann, M. W., Aramini, J. M., Kalisch, B. W., Pon, R. T., & van de Sande, J. H. (1997) *Nucleosides Nucleotides* (in press).
Gmeiner, W. H., Rayner, B., Morvan, F., Imbach, J.-L., & Lown, J. W. (1992) *J. Biomol. NMR 2*, 275−288.
Gorenstein, D. G. (1994) *Chem. Rev. 94*, 1315−1338.
Gottikh, M., Bertrand, J.-R., Baud-Demattei, M.-V., Lescot, E., Giorgi-Renault, S., Shabarova, Z., & Malvy, C. (1994) *Antisense Res. Dev. 4*, 251−258.
Guesnet, J.-L., Vovelle, F., Thuong, N. T., & Lancelot, G. (1990) *Biochemistry 29*, 4982−4991.
Harrison, R. W. (1993) *J. Comput. Chem. 14*, 1112−1122.
Harrison, R. W., & Weber, I. T. (1994) *Protein Eng. 7*, 1353−1363.
Heitman, J. (1992) *BioEssays 14*, 445−454.
Hélène, C. (1994) *Eur. J. Cancer 30A*, 1721−1726.
Koga, M., Wilk, A., Moore, M. F., Scremin, C. L., Zhou, L., & Beaucage, S. L. (1995) *J. Org. Chem. 60*, 1520−1530.
Lancelot, G., Guesnet, J.-L., Roig, V., & Thuong, N. T. (1987) *Nucleic Acids Res. 15*, 7531−7547.
Lancelot, G., Guesnet, J.-L., & Vovelle, F. (1989) *Biochemistry 28*, 7871−7878.
Lavignon, M., Tounekti, N., Rayner, B., Imbach, J.-L., Keith, G., Paoletti, J., & Malvy, C. (1992) *Antisense Res. Dev. 2*, 315−324.
Lönnberg, H., & Vuorio, E. (1996) *Ann. Med. 28*, 511−522.
Marky, L. A., Blumenfeld, K. S., Kozlowski, S. A., & Breslauer, K. J. (1983) *Biopolymers 22*, 1247−1257.
McBride, L. J., Kierzek, R., Beaucage, S. L., & Caruthers, M. H. (1986) *J. Am. Chem. Soc. 108*, 2040−2048.
Milligan, J. F., Matteucci, M. D., & Martin, J. C. (1993) *J. Med. Chem. 36*, 1923−1937.
Morvan, F., Rayner, B., Imbach, J.-L., Lee, M., Hartley, J. A., Chang, D.-K., & Lown, J. W. (1987) *Nucleic Acids Res. 15*, 7027−7044.
Mueller, L. (1987) *J. Magn. Reson. 72*, 191−197.
Paoletti, J., Bazile, D., Morvan, F., Imbach, J.-L., & Paoletti, C. (1989) *Nucleic Acids Res. 17*, 2693−2704.
Plateau, P., & Guéron, M. (1982) *J. Am. Chem. Soc. 104*, 7310−7311.
Praseuth, D., Chassignol, M., Takasugi, M., Le Doan, T., Thuong, N. T., & Hélène, C. (1987) *J. Mol. Biol. 196*, 939−942.
Rinkel, L. J., & Altona, C. (1987) *J. Biomol. Struct. Dyn. 4*, 621−649.
Rinkel, L. J., van der Marel, G. A., van Boom, J. H., & Altona, C. (1987a) *Eur. J. Biochem. 163*, 275−286.
Rinkel, L. J., van der Marel, G. A., van Boom, J. H., & Altona, C. (1987b) *Eur. J. Biochem. 163*, 287−296.
Roongta, V. A., Jones, C. R., & Gorenstein, D. G. (1990) *Biochemistry 29*, 5245−5258.
Schmieder, P., Ippel, J. H., van den Elst, H., van der Marel, G. A., van Boom, J. H., Altona, C., & Kessler, H. (1992) *Nucleic Acids Res. 20*, 4747−4751.
Séquin, U. (1973) *Experientia 29*, 1059−1062.
Sklenár, V., & Bax, A. (1987a) *J. Magn. Reson. 74*, 469−479.
Sklenár, V., & Bax, A. (1987b) *J. Am. Chem. Soc. 109*, 7525−7526.
Sklenár, V., Miyashiro, H., Zon, G., Miles, T., & Bax, A. (1986) *FEBS Lett. 208*, 94−98.
Thuong, N. T., Asseline, U., Roig, V., Takasugi, M., & Hélène, C. (1987) *Proc. Natl. Acad. Sci. U.S.A. 84*, 5129−5133.

van de Sande, J. H., Ramsing, N. B., Germann, M. W., Elhorst, W., Kalisch, B. W., Kitzing, E. V., Pon, R. T., Clegg, R. C., & Jovin, T. M. (1988) *Science 241*, 551−557.

van de Sande, J. H., Kalisch, B. W., Quong, B. Q., & Germann M. W. (1994) Antisense Oligonucleotides with Polarity and Anomeric Center Reversal, International Antisense Conference of Japan, Kyoto, December 4−7.

van Wijk, J., Huckriede, B. D., Ippel, J. H., & Altona, C. (1992) *Methods Enzymol. 211*, 286−306.

Vichier-Guerre, S., Pompon, A., Lefebvre, I., & Imbach, J.-L. (1994) *Antisense Res. Dev. 4*, 9−18.

Wagner, R. W. (1994) *Nature 372*, 333−335.

Westhof, E. (1987) *J. Biomol. Struct. Dyn. 5*, 581−600.

Wijmenga, S. S., Mooren, M. M. W., & Hilbers, C. W. (1993) in *NMR of Macromolecules; A Practical Approach* (Roberts, G. C. K., Ed.) pp 217−288, Oxford University Press, New York.

Willker, W., Leibfritz, D., Kerssebaum, R., & Lohman, J. (1993) *J. Magn. Reson., Ser. A 102*, 348−350.

Wüthrich, K. (1986) *NMR of Proteins and Nucleic Acids*, John Wiley & Sons, Inc., New York.

Zelphati, O., Imbach, J.-L., Signoret, N., Zon, G., Rayner, B., & Leserman, L. (1994) *Nucleic Acids Res. 22*, 4307−4314.

BI9706071